

# BALANCING ON THE VERTICAL SHAFT OF A FLYWHEEL ENERGY STORAGE SYSTEM

Xingjian Dai

*Tsinghua University, Department of Engineering, Beijing, China*  
email: [daixj@mail.tsinghua.edu.cn](mailto:daixj@mail.tsinghua.edu.cn)

Xi Li

*Electric Power Research Institute of Guangdong Power Grid Co., Ltd, Guangzhou, China*

Kai Zhang, Pei Liu

*Tsinghua University, Department of Engineering, Beijing, China*

A hybrid fibres composite flywheel in disk shape was connected to the shaft through a steel hub in cylindrical shell. The shaft of the flywheel and motor was supported by a permanent magnetic bearing and roller bearings in vertical installation. Both the transfer matrix method (TMM) and finite element method (FEM) were used to get the critical speed of the flywheel shaft bearing system. Spectrum analysis on the response of the vertical shaft excitation by an impact forces showed that two natural frequencies were 102 Hz and 297 Hz. The flywheel shaft was balanced on a balancing machine in horizontal supporting to get a result of vibration reduction of 75%. The field balancing was processed on the flywheel shaft at 5 different speeds after vertical installed in the flywheel energy storage system. The running speed of 7100 rpm was arrived in atmospheric environment with large wind drag loss. The charging power was estimated in the stable running after balancing.

Keywords: flywheel energy storage, vertical shaft, balancing

---

## 1. Introduction

The unbalance between the random energy consumption and the continuous production of power in large scale puts forward the emergency needs of energy storage technology which has developed quickly in recent years. Energy storage is deemed as one of the solutions for stabilizing the supply of electricity with renewable energy such as solar and wind energy due to their fluctuation performance [1-2]. There are many kinds of EES technologies, including pumped hydro-electricity storage(PHS), compressed air energy storage(CAES), different types of batteries, flywheel energy storage(FES), superconducting magnetic energy storage(SMES), and super capacitor energy storage(SCES) [3].

Flywheel energy storage systems are electro-mechanical storage devices that are composed by rotor in large rotational inertial, motor/generator, bearing, sealing chamber and power electronic interface and running monitoring instruments. In the FES operation, an electric supply charges the flywheel that stores energy in the form of kinetic energy which is based on the form, mass, and rotational speed of the flywheel [4]. The kinetic energy is maintained in the standby mode. When the stored energy is required, the FW begins to discharge the kinetic energy [5].

Flywheel energy storage has many merits such as high power density, long cycling using life, fast response, observable energy stored and environmental friendly performance. The advantageous features make FES a very suitable option for different applications such as braking energy storage

and reusing in transportation, uninterrupted power supply, frequency regulation for grid and wind power smoothing [6].

A single flywheel stored energy of 0.5-130 kWh in charging or discharging with power of 0.3-2400kW in industry application or experimental development of FES. The kinetic energy stored in a flywheel is proportional to the inertia and the square of its rotating speed designed as high as possible.

The vibration problems such as synchronic vibration from mass unbalance, passing through vibration resonance, sub-harmonic or super-harmonic vibration and stability of the rotor-bearing system become serious for high speed machine whose rotational speed is higher than multiple critical speeds [7]. Bearings technology is a key to FES. An optimal control system is proposed by incorporating cross-coupling technology into the control architecture to improve the synchronization performance of the rotor in the radial direction [8]. Squeeze film damper was employed to suppress the unbalance response and to improve the stability at high speed [9]. The transmitted force acting on the bearing housing has been analysed; the relationship between the transmitted force and the rotating speed of the rotor for the lower SFD with different oil film gaps was given [10].

For high speed rotational machinery, balancing is necessary for the smooth running. The alteration of the flywheel speed makes the balancing more difficult. The rotor is balanced at its first bending critical speed using modal balancing method in a single trial run and using a single balancing plane.[11]. Yang and Lin formulated a method for estimation of distributed unbalance of rotor using polynomial curves with finite element method for eccentricity identification of long continuous rotors [12].

In this paper, a test rig of FES system was built to investigate the composite flywheel design, bearing technology and balancing processing of rotor-bearing system running in a wide scope of rotational speed. The rotor dynamics was analysed by transfer matrix method and finite element method. The flywheel motor shaft system was hammered to get its natural frequencies in free boundary conditions. Off-line and in-situ balancing was processed on the flywheel motor bearing shaft system.

## 2. Composite flywheel motor shaft system configuration

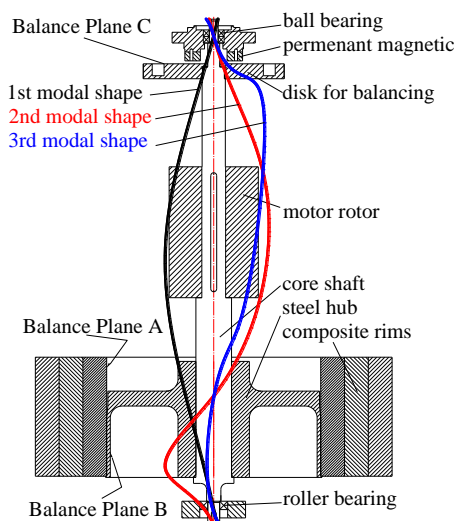


Figure 1: Flywheel rotor shaft bearing system.

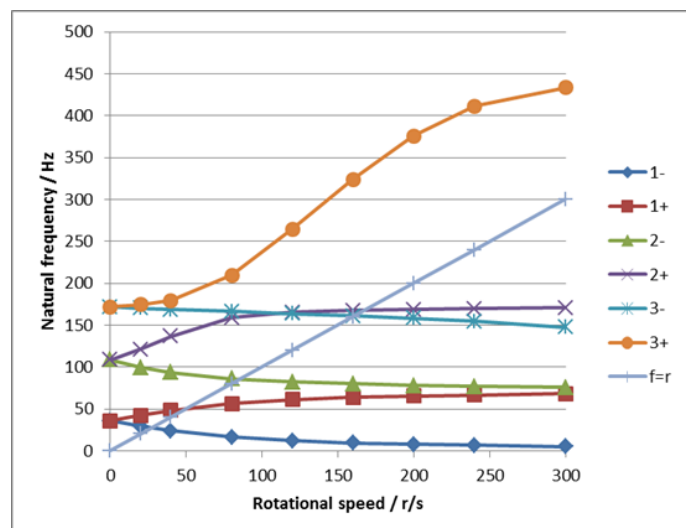


Figure 2: Natural whirl frequencies.

As shown in Fig. 1, the flywheel in disk shape is composed by three rims: the first inside rim made from glass fibre reinforced polymer, the second middle rim made from glass-carbon hybrid fibre reinforced polymer and the third rim made from carbon fibre reinforced polymer. The steel hub connects the rim and the shaft in shrink fit. The motor rotor locates in the middle of the shaft.

The top support included the magnet bearing and a pair of angular contact ball bearing. The bottom support is a cylindrical roller bearing with elastic damping block with rubber rings.

### 3. Rotordynamics analysis

Rotor dynamics analysis for high speed machinery is necessary in design and test. Critical speeds prediction, unbalance response calculation and stability boundary are essential to rotor dynamics.

#### 3.1 Transfer matrix method

While in the transfer matrix method (TMM), which is also called the Myklestand & Prohl Method, the shaft is divided into a number of imaginary smaller beam elements and governing equations are derived for each of these elements in order to determine the overall system behavior. Once we have the point and field matrices, we can use them to form the overall transfer matrix to relate the state vector at one extreme end station (i.e., the left) to the other extreme end (i.e., the right). Using the system boundary conditions, the frequency equation in the form of a polynomial is built and solved by numerical methods. The modal shape and the unbalance response also could be calculated from the transfer matrix processing. The prediction results are illustrated in Tab. 1 and Fig. 1 for different bearing stiffness values.

Table 1: Natural frequencies of the flywheel motor shaft bearing in non-rotating state

Stiffness of support N/m	$1 \times 10^7$	$3.5 \times 10^7$	$1 \times 10^8$	$3.5 \times 10^8$	$1 \times 10^9$
1st mode frequency / Hz	33.9	35.7	36.1	36.3	36.4
2nd mode frequency / Hz	78.8	108.8	126.2	135.8	138.7
3rd mode frequency / Hz	140.1	171.9	183.6	188.5	189.8

Changing the rotational speed will split the natural frequencies into backward (“-” in Fig. 2) and forward (“+” in Fig.2) whirl, which illustrated in Fig. 2 (Bearing stiffness being  $3.5 \times 10^7$  N/m). From figure 2, the first two critical speeds of the flywheel rotor shaft bearing system were found to be 3060 rpm and 10800 rpm respectively.

#### 3.2 Finite Element Method

Results from ANSYS software computation is shown in Fig. 3-6. In the case of stiffness assumed as  $3.5 \times 10^7$  N/m, the three critical speeds are 2804 rpm, 7990 rpm, and 16810 rpm. The results are different from that of TMM.

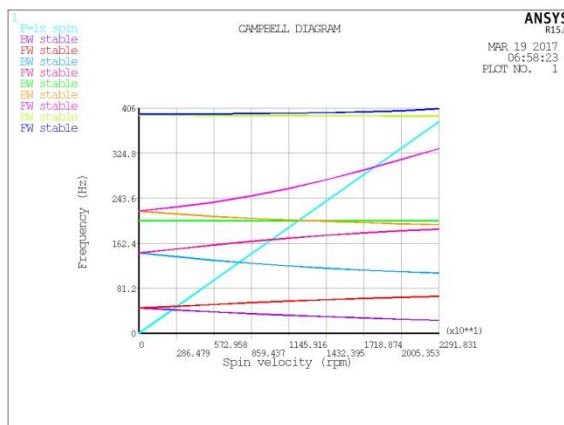


Figure 3: Natural whirl frequencies.

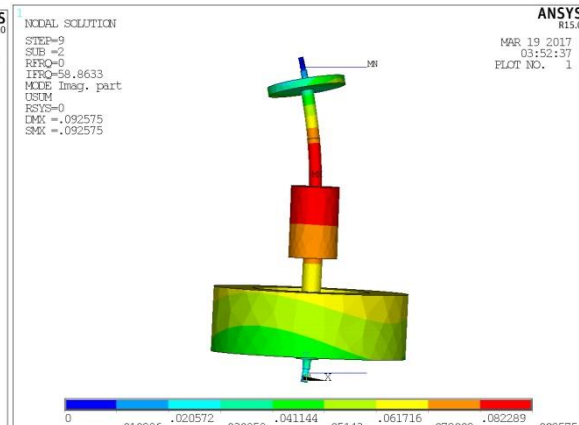


Figure 4: Modal shape.

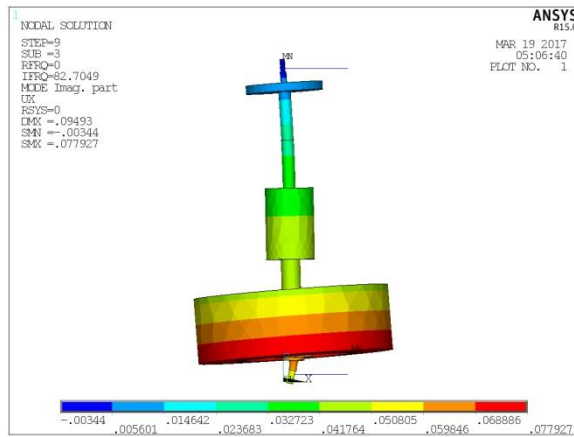


Figure 5: Modal shape.

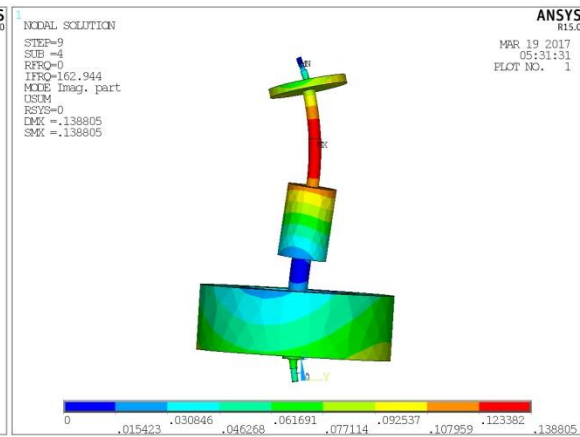


Figure 6: Modal shape.

## 4. Experimental results

Modal test is common to find the dynamics performance. Hammer impact is easy to measure the natural frequency of structure. Both the flywheel motor shaft and the FES installation casing was tested by hammer impact method. Off-line balancing was processed on the composite rim in a horizontal balancing machine. In-situ balancing procedure was completed in the vertical assembly state.

### 4.1 Natural frequency from impact response test

In the above theoretical analysis, the support stiffness is difficult to predict exactly. Therefore, modal experiment is used to help prediction the dynamics of the shaft system. A wood hamper was used to hammer the shaft in vertical suspension. The vibration was checked by a vibration signal analyser to get the response and the frequency component of the response. The main frequencies with peak component were 4Hz, 102Hz, and 297 Hz respectively (seeing Fig. 7). From this test, we can know that one critical speed of the flywheel motor shaft bearing system would be higher than 6000 rpm.

After the flywheel motor shaft system is installed vertically into the seal chamber and casing support, the impact test was done on the flywheel energy storage system casing. Three peaks were excited as 12 Hz, 32.5 Hz and 83.50 Hz (seeing Fig. 8). Therefore, the resonant vibration speed would be around 1900 rpm and 4600-5600 rpm due to the stationary mechanical structure.

From the impact test on the flywheel motor shaft system and the integrated installation machine casing, two resonant speed spans should be passed. One is around 2000-3000 rpm, the other is around 4500-6000 rpm.

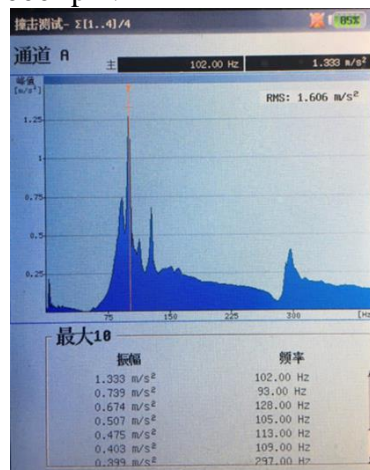


Figure 7: Vibration pick-up on the motor.

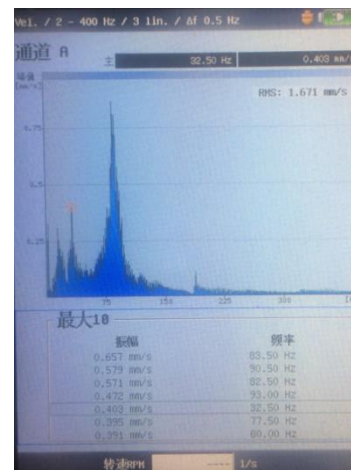


Figure 8: Vibration pick-up at the casing.

## 4.2 Off-line balancing

It is difficult to balance such a flywheel shaft due to mass location away from the middle of the shaft span and the hub structure in disk and shell form. The balance plane A and B locates near from each other (seeing Fig.1). The single plane balancing method is used to find the trial weight in plane A and B separately, and then the two planes balancing schedules are completed to get a small residual unbalance. It is necessary to using A and B balancing Plane because that the composite rim may have large unbalance being difficult to be corrected by the balancing plane C in small size.

Table 2: Plane A

Initial vibration / $\mu\text{m}$	14.9, $\angle 243^\circ$	14.9, $\angle 243^\circ$	14.9, $\angle 243^\circ$	14.9, $\angle 243^\circ$
Trial weight / g	13.7, $\angle 90^\circ$	13.7, $\angle 0^\circ$	13.7, $\angle 270^\circ$	13.7, $\angle 180^\circ$
Trial vibration / $\mu\text{m}$	9.2, $\angle 175^\circ$	12.6, $\angle 312^\circ$	28.1, $\angle 261^\circ$	27.6, $\angle 219^\circ$
Correcting Weight /g	14.3, $\angle 53^\circ$	13.0, $\angle 48^\circ$	13.9, $\angle 53^\circ$	13.5, $\angle 47^\circ$

Table 3: Plane B

Initial vibration / $\mu\text{m}$	28.6, $\angle 231^\circ$	28.6, $\angle 231^\circ$	28.6, $\angle 231^\circ$	28.6, $\angle 231^\circ$
Trial weight / g	14.2, $\angle 53^\circ$	14.4, $\angle 90^\circ$	28.3, $\angle 90^\circ$	28.3, $\angle 150^\circ$
Trial vibration / $\mu\text{m}$	17.6, $\angle 223^\circ$	23.1, $\angle 210^\circ$	22.2, $\angle 156^\circ$	41.6, $\angle 169^\circ$
Correcting Weight /g	37.5, $\angle 43^\circ$	38.5, $\angle 41^\circ$	39.0, $\angle 38^\circ$	32.8, $\angle 44^\circ$

Table 4: Two planes balancing (Plan A and Plane B)

	Plane A	Plane B
Initial vibration / $\mu\text{m}$	16.1, $\angle 240^\circ$	29.0, $\angle 232^\circ$
Trail weight / g	14.4, $\angle 53^\circ$	-
Trail weight / g	-	37.8, $\angle 43^\circ$
Correcting Weight / g	55.5, $\angle 356^\circ$	47.6, $\angle 161^\circ$
Residual vibration / $\mu\text{m}$	4.5, $\angle 37^\circ$	4.5, $\angle 223^\circ$

## 4.3 In-situ balancing

The disk element designed as the rotating ring of the permanent magnetic bearing, which was settled as the third balancing plane in-situation running in vertical state (seeing Fig. 1, Plane C). The frequencies according to the balancing processing speeds are close to the resonant frequencies of the casing in impact test above. The vibration sensors locate at the top and the bottom of the machine close to the bearings.

Table 5: Two planes balancing results

1850rpm, Correcting Weight 1 / g	21.6, $\angle 127^\circ$	22.4, $\angle 90^\circ$
4200rpm, Correcting Weight 2 / g	26.3, $\angle 60^\circ$	6.0, $\angle 110^\circ$
3900rpm, Correcting Weight 3 / g	15.2, $\angle 270^\circ$	15.3, $\angle 270^\circ$
5000rpm ,Correcting Weight 4 / g (Fig. 9)	2.07, $\angle 120^\circ$	3.15, $\angle 300^\circ$
4810rpm , Correcting Weight 5 / g (Fig. 10)	-	4.90, $\angle 245^\circ$
4810rpm, Correcting Weight 6 / g (Fig. 11)	1.44, $\angle 150^\circ$	5.30, $\angle 300^\circ$



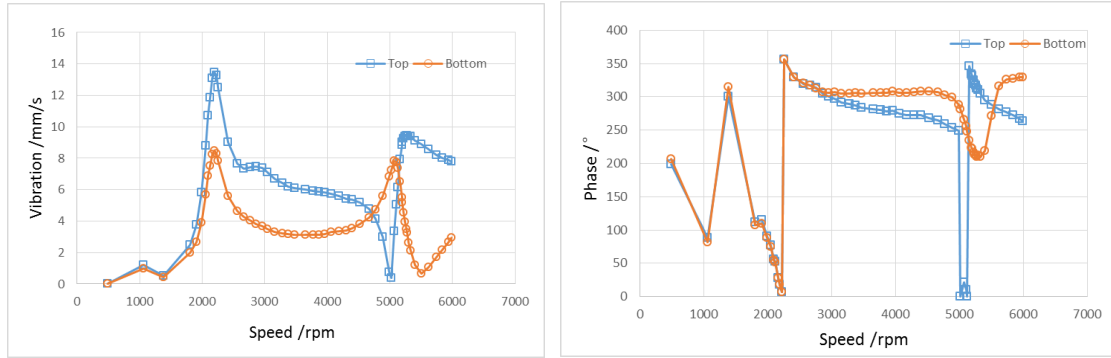


Figure 9: Unbalance response (correcting weight 4).

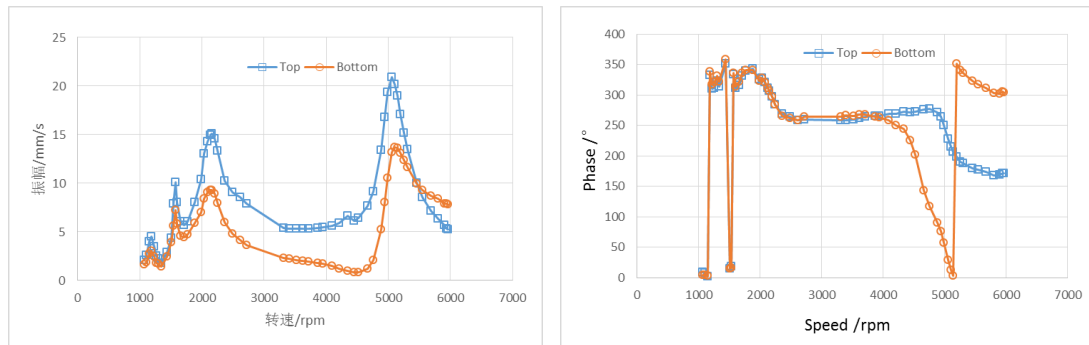


Figure 10: Unbalance response (correcting weight 5).

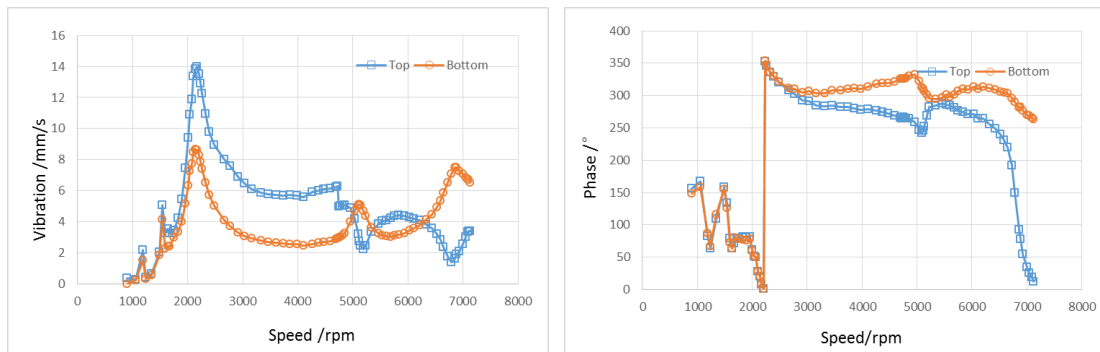


Figure 11: Unbalance response (correcting weight 6).

Comparing Fig. 9, 10, 11, we can find that correcting weight 6 is effective to suppress the vibration at the speeds between 4000-6000 rpm. The flywheel energy storage system could charge and discharge in the speed scope between 0 rpm and 7100 rpm after the balancing.

In the charging mode, it cost 6.25 seconds to increase the speed from 6750 rpm to 6850 rpm. The accelerating power is 4.8kW. In the decelerating without discharging, it cost 3.5 seconds to decrease the speed from 6850 to 6750 rpm. The decelerating power is 8.4kW mainly because of wind drag loss and bearing friction loss. Therefore, the charging power of electronic power control system is 13kW at the speed of 6800 rpm. For higher speed running test, the wind drag loss should be cut down by helium gas added into the seal chamber or running in vacuum condition.

## 5. Conclusions

The flywheel motor shaft bearing system was designed and built to do impact test and balancing test. Both the transfer matrix method and finite element method (FEM) were used to get the whirl frequencies and the critical speeds of the flywheel shaft bearing system. From the calculation, the three critical speeds are around 3000 rpm, 8000 rpm, 10800 rpm and 16000 rpm.

The vertical shaft in suspension excited by an impact forces expressed out two natural frequencies being 102 Hz and 297 Hz. The FES machine casing system was excited with peak response in frequencies as 12 Hz, 32.5 Hz and 83.50 Hz.

The flywheel shaft was balanced on a balancing machine in horizontal supporting to get a result of vibration reduction of 75%. The in-situ balancing in vertical installation was processed at 5 different speeds. The resonant speeds are around 2200 rpm and 5100 rpm being lower than the theoretical prediction. The running speed of 7100 rpm was arrived in atmospheric environment with large wind drag loss.

## REFERENCES

- 1 Evans, A., Strezov, V., Evans, T. J. Assessment of utility energy storage options for increased renewable energy penetration. *Renew Sustain Energy Rev.*, **16** (6):4141–7, (2012).
- 2 D áz-Gonz ález, F., Sumper, A., Gomis-Bellmunt, O., Villaf ñila-Robles, R. A review of energy storage technologies for wind power applications. *Renew Sustain Energy Rev.*, **5**(16):2154–71(4), (2012).
- 3 Behnam, Zakeri, Sanna, Syri. Electrical energy storage systems: A comparative life cycle cost analysis, *Renewable and Sustainable Energy Reviews*. **42**: 569–596, (2015).
- 4 Nguyen, T. D., Tseng, K. T., Zhang, S., Nguyen, H. T. A novel axial flux permanent magnet machine for flywheel energy storage system: design and analysis. *IEEE Trans Ind Electron.*, **58**(9):3784–94, (2011).
- 5 Genta, G. *Kinetic energy storage Theory and practice of advanced flywheel systems*, Butter-worth's, (1985).
- 6 Dai, X., Deng, Z., Liu, G., Tang, X., Zhang, F. and Deng, Z., Review on advanced flywheel energy storage system with large scale. *Trans China Electrotech Soc.*, **26**, 133–40, (2011).
- 7 Vance, J., Zeidan, F. and Murphy, B. *Machinery Vibration and Rotor dynamics*, John Wiley & sons, Inc., (2010).
- 8 Zhu, K.Y., Xiao, Y. and Rajendra A.U. Optimal control of the magnetic bearings for a flywheel energy storage system, *Mechatronics*, **19**(8), 1221-1235, (2009).
- 9 Dai, X., Shen, Z., Wei, H. On the vibration of rotor-bearing system with squeeze film damper in an energy storage flywheel, *International Journal of Mechanical Sciences*, **43**(11), 2525-2540, (2001).
- 10 Wang, H. C., Jiang, S. Y., Shen, Z. P. The Dynamic Analysis of an Energy Storage Flywheel System With Hybrid Bearing Support, *Journal of Vibration and Acoustics ASME*, **131**: 051006-1, (2009).
- 11 Deepthikumar, M. B., Sekhar, A. S., Srikanthan, M. R. Modal balancing of flexible rotors with bow and distributed unbalance, *Journal of Sound and Vibration*, **332**: 6216–6233, (2013).
- 12 Yang, T. C., Lin, C. Estimation of distributed unbalance of rotors, *Journal of Engineering for Gas Turbines and Power ASME*. **124**: 976–983, (2002).